

Studying of Explosive Electron Emission From “Whisker” Cathode Using X-Ray Point-Projection Radiography

Sergey A. Pikuz¹, Tatiana A. Shelkovenko, Ivan N. Tilikin, Egor V. Parkevich, Albert R. Mingaleev, Alexey V. Agafonov, and David A. Hammer², *Member, IEEE*

Abstract—The results of direct observation of the initial phase of explosive electron emission using high-resolution X-ray radiography in X-pinch radiation are reported. The confirmation of common “Ecton” theory was not found within achieved temporal and spatial resolutions. A mechanism involving the surface breakdown of whiskers that leads to plasma development is proposed.

Index Terms—Explosive electron emission (EEE), plasma, X-pinch, X-ray imaging.

I. INTRODUCTION

MOST theories of explosive electron emission (EEE) are based on the idea of cathode plasma flares developing after the explosion of fine metal filaments, or “whiskers,” on the cathode surface. According to “Ecton” theory [1], [2], the explosion of the whiskers is initiated by electron emission in a strong (10^7 – 10^8 V/cm) electric field. However, to date, the spatial structure of an electron emission flare, its origin, and the process of flare development are still a matter of conjecture. In this paper, we have used X-pinch point-projection X-ray radiography [3]–[5] to directly observe the whisker explosion in a high-current (>20 kA) diode.

II. EXPERIMENTAL SETUP

The experimental arrangement is shown in Fig. 1(a). The cathode–anode electrode gap under study, which we will call a “target diode,” was placed in one of two return current paths of hybrid X-pinch (HXPs) used as the main load on XP (500-kA output current amplitude, 100-ns rise time) and BIN (270-kA output current amplitude, 100-ns rise time)

Manuscript received December 17, 2017; revised June 4, 2018; accepted June 4, 2018. This work was supported in part by the NNSA Stewardship Sciences Academic Programs through DOE Cooperative Agreement under Grant DE-NA0003764 and in part by the Russian Science Foundation under Grant 14-22-00273. The review of this paper was arranged by Senior Editor F. Beg. (*Corresponding author: Sergey A. Pikuz.*)

S. A. Pikuz, T. A. Shelkovenko, and D. A. Hammer are with the Laboratory of Plasma Studies, Cornell University, Ithaca, NY 14850 USA (e-mail: pikuz@yahoo.com; taniashel@yahoo.com; dah5@cornell.edu).

I. N. Tilikin, E. V. Parkevich, A. R. Mingaleev, and A. V. Agafonov are with the P. N. Lebedev Physical Institute of Russian Academy of Sciences, 119991 Moscow, Russia (e-mail: ivan.tilikin@gmail.com; v754@rambler.ru; albert99@inbox.ru; agafonov@lebedev.ru).

Color versions of one or more of the figures in this paper are available online at <http://ieeexplore.ieee.org>.

Digital Object Identifier 10.1109/TPS.2018.2852058

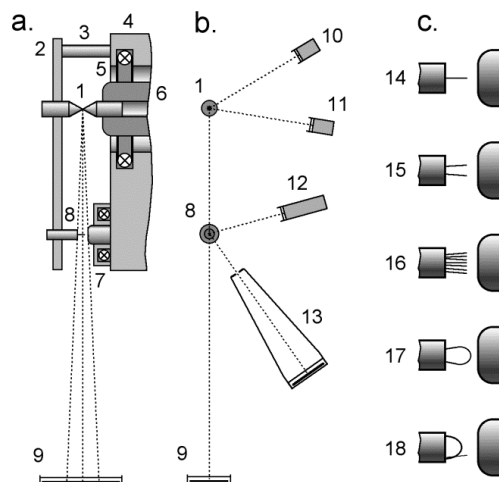


Fig. 1. Experimental arrangement. (a) Side view (1: HXP, 2: X-pinch anode, 3: return-current post, 4: pulser ground, 5: total current Rogowsky, 6: X-pinch cathode, 7: target diode current Rogowsky, 8: target diode). (b) Front view (9: film pack, 10: PCD with 25- μ m Be filter, 11: PCD with 12.5 or 25- μ m Ti filter, 12: AXUVHS5 silicon diode with Al filter), 13: cassette with pinhole followed by image plate. (c) Target diode whisker configurations (14: single wire sticking out from the cathode, 15: double-wire cathode, 16: multiwire cathode, 17: W wire loop cathode, 18: W wire loop cathode with a short W filament mounted on it).

pulsers [3]. The target diode current was in the range 20–150 kA depending on return circuit inductive division. Target diode cathode whiskers in different configurations, shown in Fig. 1(b), were made from thin 5–50- μ m W, Cu, or Mo wires. The radiographs shown in Figs. 2–5 were obtained in filtered (12.5- μ m Ti filter) HXP X-ray radiation with a geometric magnification of about 10 on Kodak DR50 film. The X-pinch radiation was monitored with subnanosecond time resolution using photoconducting diodes (PCDs) with 25- μ m Be and 12.5- μ m Ti filters. In some experiments, the X-pinch produced more than one X-ray pulse that was separated in time, enabling us to observe the development of a whisker explosion in one experiment, as illustrated in Fig. 2(f) together with Fig. 3(b). Time-integrated images of the target diode were recorded on Fuji TR image plates in XUV radiation using open pinholes with aperture 50 μ m. These plates do not have a plastic protective layer and are sensitive over a wide spectral range including the XUV. The hard X-ray

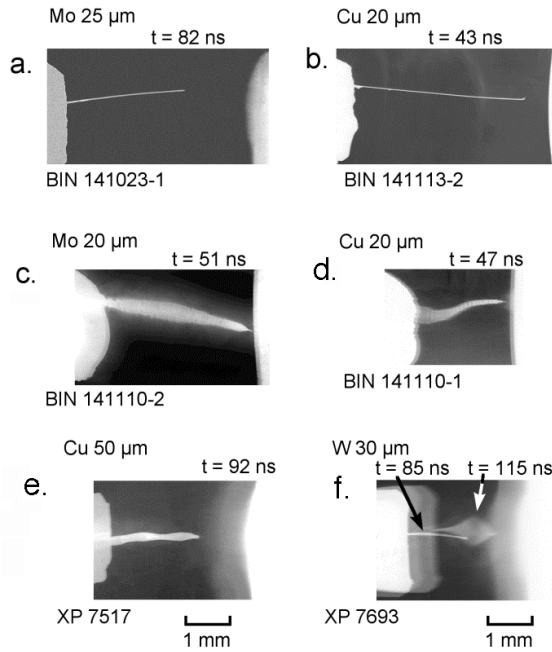


Fig. 2. (a)–(d) Radiographs of the target diodes with single-filament cathodes in experiments on BIN and (e) and (f) XP pulsers with different distances from filament tip and anode.

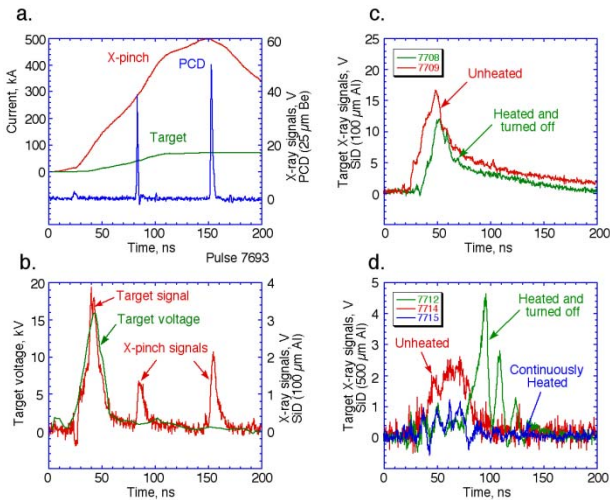


Fig. 3. Examples of the signals recorded in the experiments on the XP pulser. (a) HXP (50- μm Ag) current (red), target diode current (green), and X-ray signals (blue) on the PCD with 25- μm Be filter. (b) Target diode voltage (green) and hard X-ray signals (red) from the target diode (first pulse), scattered X-ray signals from the main load (HXP) was also seen in this experiment). (c) Target hard X-ray signals from unheated loop cathode (red) and heated loop cathode (green) in energy band $E > 7$ keV (100- μm Al filter). (d) Target hard X-ray signals from unheated loop cathode (red), heated loop cathode (green), and continuously heated loop cathode (blue) in the energy band $E > 11$ keV (AXUVH55 diode with 500- μm Al filter).

radiation from the target diode was monitored by silicon diodes (AXUVH55) with Al filters (100- or 500- μm Al). Five whisker configurations were tested in the target diode as shown in Fig. 1(c)—14: a single filament, 15: double filament, 16: multifilament, 17: unheated and heated tungsten loops, and 18: unheated and heated loops together with a short and thin tungsten filament.

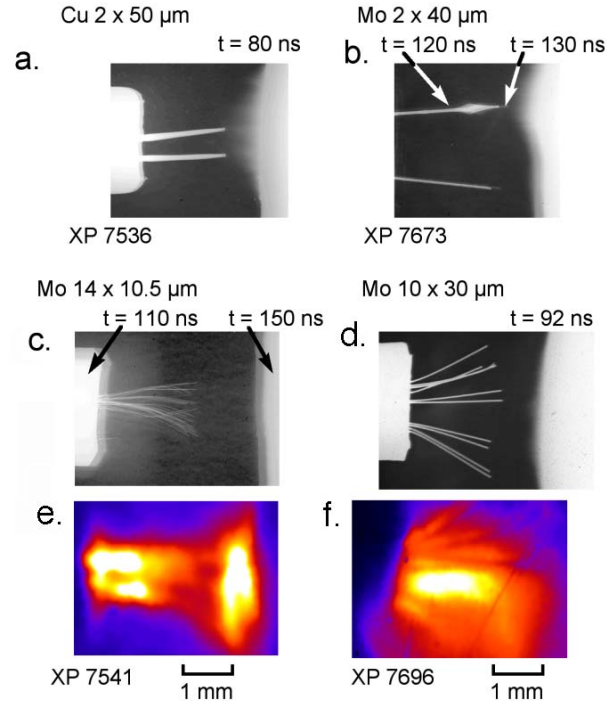


Fig. 4. (a) and (b) Radiographs of target diodes with double filament and (c) and (d) multifilament cathodes in experiments on the XP pulser; (e) and (f) Open pinhole time-integrated images in the XUV spectral band of the multifilament tests shown in (c) and (d).

III. EXPERIMENTAL RESULTS

In the first experiments on the BIN pulser with the single filament on the cathode [6], we did not observe any wire explosion if the gap between a wire tip and the anode exceeded 0.5–1 mm [Fig. 2(a) and (b)] for all the wire material tested. However, in all the experiments, X-ray signals were recorded, indicating the presence of an energetic electron beam. In addition, in most tests, the e-beam left an imprint in the anode material. If the filament tip—anode distance was shortened to 50–200 μm [Fig. 2(c) and (d)], the wire radiograph showed it to be an exploded wire dense core, as was seen in exploding wire experiments [5], [7]–[10]. In experiments on the XP pulser, where the voltage applied to the target diode was higher because of the larger rate of increase of current, dI/dt , similar target diode structure was observed in radiographs when the filament tip—anode distance was less than 0.7 mm [Fig. 2(e) and (f)]. If HXP produced two or more hot spots well separated in time [Fig. 3(b)], sequentially recorded images on the same film showed different stages of the filament explosion [Fig. 2(f)]. In particular, in the first image of the 30- μm W filament [Fig. 2(f), $t = 85$ ns from the current start] one can see the unexploded filament, while in the second image ($t = 115$ ns), a substantial expansion of the filament dense core is clearly seen except at the tip.

The hard X-ray radiation from the target diode was recorded using the silicon diodes with Al filters. In the first experiments, signals from scattered (or passed through shield) hard X-ray radiation generated in the X-pinch were seen [Fig. 3(b)].

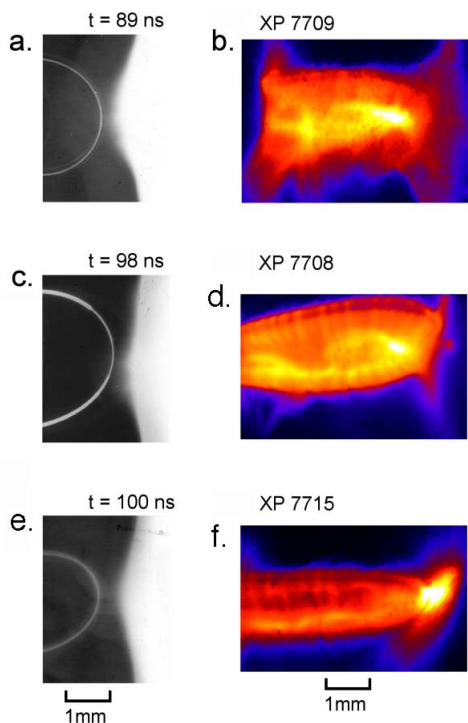


Fig. 5. Radiographs of target diodes in experiments on the XP pulser with (a) unheated, (c) heated and cooled before the shot, and (e) continuously heated 30- μm loop cathodes. (b), (d), and (f) Open pinhole time-integrated images in the XUV spectral band of corresponding the loop cathodes in (a), (b), and (c), respectively.

When additional careful shielding of the detector was done these signals disappeared. In all the experiments, both on BIN and XP, target diode hard X-ray signals corresponded to the voltage measured on the target diode. The target voltage was measured by shielded resistive divider connected to the electrodes of target diode. Unfortunately, due to high noise level and difficulties in subtracting inductive component of the signals voltage amplitudes were measured with relatively big error (about 50%).

In experiments on the XP pulser with double filament cathodes, we have seen very small core expansion [Fig. 4(a)] or expansion at very late time [Fig. 4(b)]. In the cases of multifilament (brush type) cathodes, the expansion of filament cores was not seen at any time that we could view with X-ray radiography ($t < 160$ ns) in our experiment even with very thin Mo wires (10.5 μm). Visible diameters of the filament cores were equal to the initial “cold” wire diameters within the experimental spatial resolution of point-projection radiography [5] (2–3 μm in these experiments).

Time-integrated images recorded using open pinholes with Fuji TR image plates, taking advantage of their sensitivity in the XUV spectral band ($100 \text{ eV} < E < 1000 \text{ eV}$) showed the presence of cathode plasmas, with dense filament cores present the entire time cathode plasmas were visible. This time exceeds the time of e-beam generation and is equal to the time of current flowthrough the target diode. Shadows of the dense cores are clearly seen on the images in Fig. 4(e) and (f). The existence of long-lived dense cores in the filament plasmas is

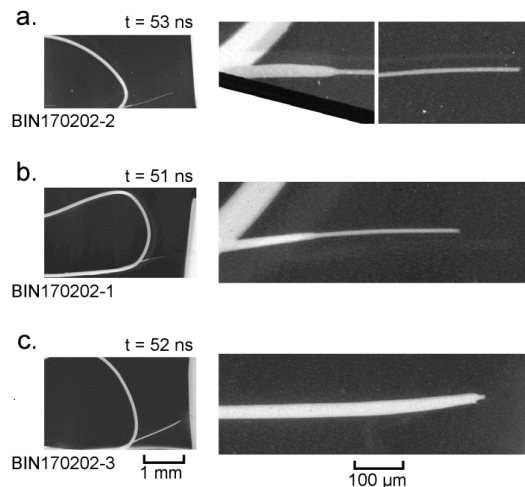


Fig. 6. Radiographs of the target diodes in experiments on the BIN pulser with (a) unheated, (b) heated and cooled before the shot, and (c) continuously heated 100- μm W loop cathodes with 10- μm W whiskers, showing expanded views of the whiskers at the indicated times.

similar to that in wire arrays during the ablation phase [10]. It is reasonable to suppose that the cathode plasma appearance is connected with the filament surface breakdown.

The simplest way to change cathode surface conditions is to clean the surface by heating to high temperature in vacuum. In an experiment by Zakharov *et al.* [11] 30 years ago, a sharp-edge tube cathode pulsed to high voltage (400 kV) for 4 μs in a magnetically insulated diode was replaced by a heated W wire loop that was done to improve the electron beam stability and extend the duration of magnetic insulation. Instead, continuous heating to the temperature of about 1600 K reduced electron emission by two orders of magnitude. In the present experiments, the filament cathode was replaced by a W loop, which could then be heated to the temperature ≈ 1300 –1600 K. Without loop heating, the discharge in the target diode was very similar to ones with single and multifilament cathodes [Fig. 5(a) and (b)]. No filament explosion was observed in radiographs, and the cathode plasma had similar precursor-like structure. If the W loop was heated but disconnected from electric circuit just before the shot to decrease the risk of power supply damage, the partial expansion of the filament core became visible and the image of the cathode plasma became more stable. X-ray signals in the photon energy band $E > 7$ keV were not very different in the two cases, but in higher energy bands (where signal amplitudes were an order of magnitude smaller) in the diode with heated cathode, X-ray signals appeared 40 ns later than in unheated [see Fig. 3(c) and (d)]. If the cathode loop was heated continuously (additional protection of power supply was added to the circuit) to the temperature ≈ 1600 °K, the hard X-ray signal practically disappeared into the noise and the image of the loop core becomes “fuzzy” but does not appear to be exploded.

The loop cathode does not model a cathode with whiskers very well and the more realistic cathode design used on BIN pulser is shown in Fig. 6. A 100- μm W loop was used as the

heater for a 10- μm W whisker wrapped around the 100- μm wire. In these experiments, no explosion of the whiskers was observed. Only in the case of a continuously heated cathode was there clearly visible expansion (not explosion!) of most of the whisker (but, again, not near the whisker tip). In all other cases, there was no whisker explosion along most of the whisker. X-ray signals in $E > 7$ keV energy band were very similar in all experiments to those obtained in experiments on XP.

All of the experimental results described earlier show the absence of an explosion of filament or whisker cathodes in the target diodes upon application of anode voltages in the range 20–80 kV during e-beam generation. The implied electric field is 10^7 – 10^8 V/cm. The behavior of the whiskers looks more like wire explosion with the development of well-known core–corona structure that would mean that is a breakdown on the wire surface of the metal vapor or adsorbed gas at a certain moment, at which time the discharge current transfers to the coronal plasma surrounding the wire cores [12]–[15].

There are number of possible scenarios of EEE related to the experimental results obtained in our experiments.

- 1) *Ecton Scenario*: Whiskers on the cathode surface are exploded by the current from electron field emission, producing a plasma flare as an unlimited source of electrons. The whiskers disappear at the beginning of the applied voltage pulse, leaving behind small craters on the cathode surface [1], [2].
- 2) *Electron Field-Emission Shunting*: Due to the nonuniform electric field strength, electron field emission is nonuniform along the whisker (filament/wire in our case) producing nonuniform energy deposition in the wire. This must result in nonuniform wire core expansion, increasing from the tip to the foot. Expansion of the core must start shortly after the beginning of electron emission and must smoothly increase from the tip to the foot of the wire. Whisker explosion follows, producing cathode plasma and space-charge-limited electron flow. This scenario was proposed and analyzed in [16].
- 3) *Surface Breakdown*: Field emission from the filament tip initiates the breakdown of adsorbed gases and debris that desorb from the filament surface, or perhaps from filament mate. The core will expand only after surface breakdown occurs and so expansion, in this case, will be nonuniform since the breakdowns along different parts of the filament may occur at different times. This scenario is very similar to discussed one in [17] for the EEE from the velvet cathode.
- 4) *Exploded Wire*: The whisker (filament) produces a field-emitted electron beam (from the wire tip and wire surface) and this beam produces a plasma flare on the anode. Anode plasma shorts out the filament–anode gap, connecting the filament directly to the anode, after which the filament behavior will be identical to the behavior of an exploded wire. This scenario depends upon the fact that the process is critically dependent on the filament tip–anode gap. The typical rate of anode plasma expansion is $(5\text{--}10) \times 10^5$ cm/s, while the radiography exposure time varied from 40 to 110 ns

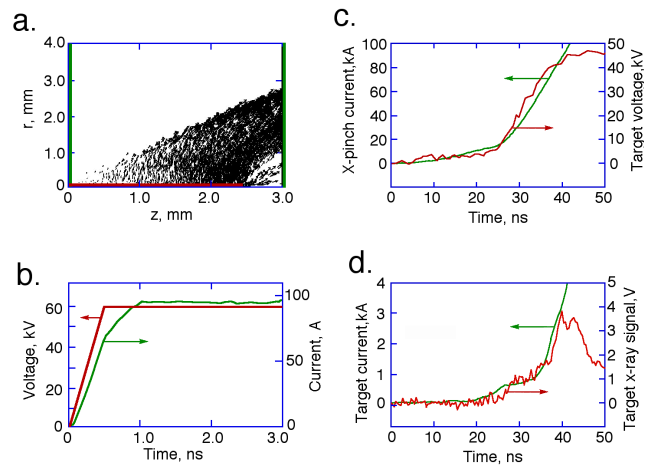


Fig. 7. Modeling of the electron beam propagation using KARAT code and experimental results with 30- μm W single pin cathode (pulse XP7639). (a) Map of electron flow at $t = 3$ ns. Green lines: electrodes positions. Red line: pin cathode. (b) Voltage and current at the same time. (c) X-pinch current and target diode voltage. (d) Target diode current and X-ray signal through 100- μm Al filter.

after the current start on BIN pulser and from 80 to 150 ns on the XP pulser. Surface breakdown time is about 10–30 ns and depends on the voltage applied to the target diode at the moment of filament–anode gap closure. That means the visible expansion of dense cores can be seen in our experiments if the filament–anode distance does not exceed 1 mm.

We have modeled a discharge in a target diode with a filament cathode and a flat anode using the electrodynamic code KARAT [18]. Results are shown in Fig. 7 together with some experimental results from a similar configuration. We assume a 50- μm W filament is placed with its tip 550 μm from the anode [Fig. 7(a)]. With field emission only, the discharge current was limited by the space charge to less than 100 A upon application of an anode voltage 60 kV [Fig. 7(b)]. This is significantly less than the measured current of 1–5 kA in the experiment [Fig. 7(c) and (d)]. Such currents can be achieved if the diameter of the electron-emitting surface is increased to 1–2 mm. That means that plasma developed from a surface plasma much bigger than the 550- μm filament must be the electron source. This 1–2 mm diameter is the characteristic diameter of coronal plasmas that surround exploding wires [13]–[15]. An additional argument that supports this conclusion is the fact that adding filaments combined in the form of a small diameter brush (1–2 mm) does not lead to a significant increase of the diode current, and the emitting plasma is located inside brush only. The details of simulations will be presented elsewhere.

IV. DISCUSSION AND CONCLUSION

In our experiments, we did not find support for the “Ecton” hypothesis even when the electric field strength reached 10^8 V/cm near the whisker tip, at least in the spatial scale achieved. The behavior of the whisker cathode looks more like a wire surface breakdown accompanied by wire explosion and core–corona structure development. Substantial mitigation of the

electron emission was observed in experiments with heated cathodes.

We suppose that most visible effects (light emission from flashing spots and remaining craters [1], [2], [19]–[27]) declared as confirmations of “Ecton” theory have secondary or “post effects” nature. Real sources of electron emission especially in the initial phase of discharges are connected with rare plasma developed during the surface breakdown of pins and whiskers on the cathode like it was discussed for the velvet cathodes [17]. While the explosion of sharp structures and whiskers on the cathode surface is still possible, it appears to be on the nanometer spatial range. However, if this occurs, such explosions will serve as triggers for the surface breakdown on a larger scale. To confirm or deny this statement more experiments with higher spatial resolution are needed.

REFERENCES

- [1] G. A. Mesyats and D. I. Proskurovsky, *Pulsed Electrical Discharge in Vacuum*. Berlin, Germany: Springer-Verlag, 1989.
- [2] G. A. Mesyats, “Ecton mechanism of the cathode spot phenomena in a vacuum arc,” *IEEE Trans. Plasma Sci.*, vol. 41, no. 4, pp. 676–694, Apr. 2013.
- [3] S. A. Pikuz, T. A. Shelkovenko, and D. A. Hammer, “X-pinch. Part I,” *Plasma Phys. Rep.*, vol. 41, no. 4, pp. 291–342, 2015.
- [4] S. A. Pikuz, T. A. Shelkovenko, and D. A. Hammer, “X-pinch. Part II,” *Plasma Phys. Rep.*, vol. 41, no. 6, pp. 445–491, 2015.
- [5] T. A. Shelkovenko, S. A. Pikuz, and D. A. Hammer, “A review of projection radiography of plasma and biological objects in X-pinch radiation,” *Plasma Phys. Rep.*, vol. 42, no. 3, pp. 226–268, 2016.
- [6] E. V. Parkevich *et al.*, “High-resolution X-ray projection radiography of a pin cathode in a high-current vacuum diode using X-pinch radiation,” *JETP Lett.*, vol. 103, no. 5, pp. 357–361, 2016.
- [7] D. H. Kalantar and D. A. Hammer, “Observation of a stable dense core within an unstable coronal plasma in wire-initiated dense Z-pinch experiments,” *Phys. Rev. Lett.*, vol. 71, no. 23, pp. 3806–3809, 1993.
- [8] G. V. Ivanenkov, A. R. Mingaleev, S. A. Pikuz, D. A. Hammer, and T. A. Shelkovenko, “X-ray backlighting of high-current multiwire liner discharges,” *Plasma Phys. Rep.*, vol. 25, no. 10, pp. 783–793, 1999.
- [9] S. A. Pikuz, T. A. Shelkovenko, D. B. Sinars, J. B. Greenly, Y. S. Dimant, and D. A. Hammer, “Multiphase foamlike structure of exploding wire cores,” *Phys. Rev. Lett.*, vol. 83, no. 21, pp. 4313–4316, 1999.
- [10] S. V. Lebedev *et al.*, “Effect of core-corona plasma structure on seeding of instabilities in wire array Z pinches,” *Phys. Rev. Lett.*, vol. 85, no. 1, pp. 98–101, 2000.
- [11] S. M. Zakharov, S. A. Pikuz, and V. M. Romanova, “Stability of heated tungsten wire against explosive emission,” *Soviet Phys.-Tech. Phys.*, vol. 34, no. 6, pp. 690–691, 1989.
- [12] S. I. Tkachenko *et al.*, “Analysis of the discharge channel structure upon nanosecond electrical explosion of wires,” *Phys. Plasmas*, vol. 14, no. 12, p. 123502, 2007.
- [13] S. I. Tkachenko *et al.*, “Study of the core-corona structure formed during the explosion of an aluminum wire in vacuum,” *Plasma Phys. Rep.*, vol. 38, no. 1, pp. 1–11, 2012.
- [14] A. G. Rousskikh, V. I. Oreshkin, A. Zhigalin, I. I. Beilis, and R. B. Baksht, “Expansion of the plasma corona from a wire exploded in vacuum,” *Phys. Plasmas*, vol. 17, no. 3, p. 033505, 2010.
- [15] P. U. Duselis and B. R. Kusse, “Experimental observation of plasma formation and current transfer in fine wire expansion experiments,” *Phys. Plasmas*, vol. 10, no. 3, pp. 565–568, 2003.
- [16] G. A. Mesyats, E. V. Parkevich, S. A. Pikuz, and M. I. Yalandin, “Shunting effect in explosive electron emission,” *Doklady Phys.*, vol. 61, no. 10, pp. 481–484, 2016.
- [17] R. B. Miller, “Mechanism of explosive electron emission for dielectric fiber (velvet) cathodes,” *J. Appl. Phys.*, vol. 84, no. 7, pp. 3880–3889, 1998.
- [18] V. P. Tarakanov, “User’s manual of code karat,” Berkeley Teseach Assoc., Springfield, VA, USA, Tech. Rep., 1992, p. 127.
- [19] T. A. Spencer, M. C. Clark, and A. Fisher, “Novel cathode for field-emission applications,” *Rev. Sci. Instrum.*, vol. 66, no. 3, pp. 2528–2532, 1995.
- [20] E. Garate *et al.*, “Novel cathode for field-emission applications,” *Rev. Sci. Instrum.*, vol. 66, no. 3, pp. 2528–2532, 1995.
- [21] J. M. Parson, C. F. Lynn, J. J. Mankowski, A. A. Neuber, and J. C. Dickens, “Emission behavior of three conditioned carbon fiber cathode types in UHV-sealed tubes at 200 A/cm²,” *IEEE Trans. Plasma Sci.*, vol. 42, no. 2, pp. 3982–3988, Dec. 2014.
- [22] J. M. Parson, J. J. Mankowski, J. C. Dickens, and A. A. Neuber, “Imaging of explosive emission cathode and anode plasma in a vacuum-sealed vircator high-power microwave source at 250 A/cm²,” *IEEE Trans. Plasma Sci.*, vol. 42, no. 10, pp. 2592–2593, Oct. 2014.
- [23] G. Shafir *et al.*, “Experimental research of different plasma cathodes for generation of high-current electron beams,” *J. Appl. Phys.*, vol. 118, no. 19, p. 193302, 2015.
- [24] Y. Li, Y. Sun, D. A. Jaffray, and J. T. W. Yeow, “Coulomb explosion of vertically aligned carbon nanofibre induced by field electron emission,” *RSC Adv.*, vol. 7, no. 64, pp. 40470–40479, 2017.
- [25] Y. Hua, H. Wan, X. Chen, B. Chen, P. Wu, and S. Bai, “Influence of surface microstructures on explosive electron emission properties for graphite cathodes,” *IEEE Trans. Plasma Sci.*, vol. 45, no. 6, pp. 959–968, Jun. 2017.
- [26] R. Chandra *et al.*, “Explosive emission properties of cathode materials in relativistic electron beam generation,” *IEEE Trans. Plasma Sci.*, vol. 42, no. 11, pp. 3491–3497, Nov. 2014.
- [27] H. T. C. Kaufmann, M. D. Cunha, M. S. Benilov, W. Hartmann, and N. Wenzel, “Detailed numerical simulation of cathode spots in vacuum arcs: Interplay of different mechanisms and ejection of droplets,” *J. Appl. Phys.*, vol. 122, no. 16, p. 163303, 2017.

Authors’ photographs and biographies not available at the time of publication.